 CMES, vol.8, no.1, pp.73-90, 2005

Dual Boundary Element Method for Instability Analysis of Cracked Plates

J. Purbolaksono[1] and M. H. Aliabadi[2,3]

Abstract: This paper presents the dual boundary integral equations for the buckling analysis of the shear deformable cracked plates. The domain integrals which appear in this formulation are transferred to boundary integrals using the dual reciprocity method. The plate buckling displacement and hypersingular traction integral equations are presented as a standard eigenvalue problem, which would allow direct evaluation of the critical load factor and buckling modes. Several examples with different geometries and boundary conditions are presented to demonstrate the accuracy of the proposed formulation.

keyword: Buckling, Mindlin Plate, fracture mechanics, hypersingular integral equation

1 Introduction

Boundary element method is a powerful numerical tool for general stress analysis of crack problems. The difficulty which appears in modelling of crack problems is due to coincidence of the crack surfaces that makes point collocations on two crack surfaces generate identical equations [Aliabadi (2002)]. To overcome this difficulty the dual boundary element method [Portela, Aliabadi and Rooke (1992), Mi and Aliabadi (1992)].

During the last decade, the Dual Boundary Element Method (DBEM) has been established as a robust numerical method for fracture mechanics problems. Based on displacement and traction integral equations, DBEM has been applied to many fracture mechanics problems e.g. elastostatics, thermoelastic, elastoplastic, stiffened panels, concrete cracking, composite materials and dynamics, as reviewed by [Aliabadi (1997a), (1997b)]. Applications of the dual boundary element method to fracture mechanics analysis of cracked shear deformable plates can be found in [Dirgantara and Aliabadi (2000), Dirgantara and Aliabadi (2001), Wen, Aliabadi and Young (2000)].

Application of the boundary element method to instability of plate structures has been reported by [O'Donoghue and Atluri (1987), Zhang and Atluri (1988), Syngellakis and Elzein (1994), Nerantzaki and Katsikadelis (1996)] and more recently by [Purbolaksono and Aliabadi (2005)]. Buckling analysis of cracked panels has been investigated by only few researchers analytically and numerically. [Stahl and Keer (1972)] studied stability of simply supported rectangular cracked plates using an analytical approach. [Vafai and Estekanchi (2002)] investigated the buckling behaviour of edge cracked plated subjected to axial loads. [Liu (2001)] presented the buckling analysis of rectangular Mindlin plates having cracks using differential quadrature element method.

In this paper, a new dual boundary element method for the buckling analysis of the Reissner shear deformable cracked plate is presented. The method is an extension of the boundary integral equations formulation recently presented by the authors [Purbolaksono and Aliabadi (2005)] for modelling general buckling of shear deformable plates. The domain integrals which appear in the formulation are transferred to boundary integrals using the dual reciprocity method. The plate buckling displacement and hypersingular traction equations are presented as a standard eigenvalue problem, which would allow direct evaluation of the critical load factor and buckling modes. Several examples with different geometries and boundary conditions are presented to demonstrate the accuracy of the formulation.

2 Governing Equations

The governing differential equations for plate buckling analysis can be written as:

$$M_{\alpha\beta,\beta} - Q_\alpha = 0 \tag{1}$$

[1] Department of Engineering, Queen Mary, University of London, Mile End Road, London E1 4NS, UK.

[2] Correspondence to: Ferri Aliabadi, Department of Aeronautics, Faculty of Engineering, Imperial College London, South Kensington, SW7 2BY, UK. Email address: m.h.aliabadi@imperial.ac.uk

[3] Department of Aeronautics, Imperial College London, Prince Consort Road, South Kensington, London, SW7 2BY, UK.

$$Q_{\alpha,\alpha} + (N_{\alpha\beta} w_{3,\beta})_{,\alpha} + q = 0 \tag{2}$$

$$N_{\alpha\beta,\beta} = 0 \tag{3}$$

where,

$$M_{\alpha\beta} = \frac{1-\nu}{2} D(w_{\alpha,\beta} + w_{\beta,\alpha} + \frac{2\nu}{1-\nu} w_{\gamma,\gamma}\delta_{\alpha\beta}) \tag{4}$$

$$Q_\alpha = C(w_\alpha + w_{3,\alpha}) \tag{5}$$

$$N_{\alpha\beta} = \frac{1-\nu}{2} B(u_{\alpha,\beta} + u_{\beta,\alpha} + \frac{2\nu}{1-\nu} u_{\gamma,\gamma}\delta_{\alpha\beta}) \tag{6}$$

$B = Eh/(1-\nu^2)$ is known as the tension stiffness; $D = Eh^3/\left[12\left(1-\nu^2\right)\right]$ is the bending stiffness of the plate; $C = \left[D(1-\nu)\lambda^2\right]/2$ is the shear stiffness; $\lambda = \sqrt{10}/h$ is shear factor; h is the thickness of the plate; ν is Poisson's ratio; $N_{\alpha\beta}$ are stress resultants for two-dimensional plane stress elasticity; Q_α and $M_{\alpha\beta}$ are stress resultants plate bending problems; u_α and w_3 are translation of displacements in x_1, x_2 (in-plane) and x_3 (out of plane), w_α are rotations in x_α direction; and $\delta_{\alpha\beta}$ is the Kronecker delta function. Indicial notation is used throughout this paper. Greek indices will vary from 1 to 2 and Roman indices from 1 to 3.

3 The Dual Boundary Integral Equations

A cracked body shown in Figure 1 is considered with Γ^+ and Γ^- referring to the upper and lower crack surfaces respectively, and Γ_b denotes the rest of the boundary. As the source point $\mathbf{x}^+$ is coincident with $\mathbf{x}^- \in \Gamma^-$, extra free terms $\frac{1}{2}u_\alpha(\mathbf{x}^-)$ and $\frac{1}{2}w_j(\mathbf{x}^-)$ will appear in equations (7) and (8) [see Aliabadi (2000)]. The collocation at $\mathbf{x}^-$ will also give the same integral equations as equations (7) and (8). This situation will provide an ill-conditioned system of algebraic equations. The boundary integrals of the displacement components u_α and w_i for collocation points at $\mathbf{x}^+$ on the upper crack surface Γ^+ are written as follows

$$\begin{aligned}&\frac{1}{2}u_\theta(\mathbf{x}^+) + \frac{1}{2}u_\theta(\mathbf{x}^-) + \int_\Gamma T^*_{\theta\alpha}(\mathbf{x}^+,\mathbf{x})u_\alpha(\mathbf{x})d\Gamma \\ &= \int_\Gamma U^*_{\theta\alpha}(\mathbf{x}^+,\mathbf{x})t_\alpha(\mathbf{x})d\Gamma\end{aligned} \tag{7}$$

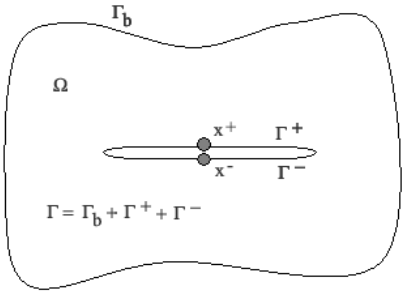

Figure 1 : A cracked body.

and

$$\begin{aligned}&\frac{1}{2}w_i(\mathbf{x}^+) + \frac{1}{2}w_i(\mathbf{x}^-) + \int_\Gamma P^*_{ij}(\mathbf{x}^+,\mathbf{x})w_j(\mathbf{x})d\Gamma \\ &\quad = \int_\Gamma W^*_{ij}(\mathbf{x}^+,\mathbf{x})p_j(\mathbf{x})d\Gamma \\ &\quad + \lambda\int_\Omega W^*_{i3}(\mathbf{x}^+,\mathbf{X})(N_{\alpha\beta,\alpha}w_{3,\beta} + N_{\alpha\beta}w_{3,\beta\alpha})d\Omega \\ &\quad + \lambda\int_\Omega W^*_{i3}(\mathbf{x}^+,\mathbf{X})q(\mathbf{X})d\Omega\end{aligned} \tag{8}$$

where $\int$– denotes the Cauchy principal value integral; $T^*_{\theta\alpha}$, $U^*_{\theta\alpha}$, P^*_{ij} and W^*_{ij} are the fundamental solutions and are listed in Appendix A.

The in-plane stress resultants at domain point X' are written as

$$\begin{aligned}N_{\alpha\beta}(\mathbf{X}') &= \int_\Gamma U^*_{\alpha\beta\gamma}(\mathbf{X}',\mathbf{x})t_\gamma(\mathbf{x})d\Gamma \\ &\quad - \int_\Gamma T^*_{\alpha\beta\gamma}(\mathbf{X}',\mathbf{x})u_\gamma(\mathbf{x})d\Gamma\end{aligned} \tag{9}$$

The deflection w_3 at the domain points X' is required as an additional equation to arrange an eigenvalue equation as follows:

$$\begin{aligned}w_3(\mathbf{X}') &= \int_\Gamma W^*_{3j}(\mathbf{X}',\mathbf{x})p_j(\mathbf{x})d\Gamma \\ &\quad - \int_\Gamma P^*_{3j}(\mathbf{X}',\mathbf{x})w_j(\mathbf{x})d\Gamma \\ &\quad + \lambda\int_\Omega W^*_{33}(\mathbf{X}',\mathbf{X})q(\mathbf{X})d\Omega \\ &\quad + \lambda\int_\Omega W^*_{33}(\mathbf{X}',\mathbf{X})(N_{\alpha\beta,\alpha}w_{3,\beta} + N_{\alpha\beta}w_{3,\beta\alpha})d\Omega\end{aligned} \tag{10}$$

The traction integral equations is used for collocations at $\mathbf{x}^- \in \Gamma^-$. For collocations on $\mathbf{x}^- \in \Gamma^-$, the in-plane stress

resultants boundary integral equation can be expressed as

$$\frac{1}{2}N_{\alpha\beta}(\mathbf{x}^-)+\frac{1}{2}N_{\alpha\beta}(\mathbf{x}^+)+\oint_\Gamma T^*_{\alpha\beta\gamma}(\mathbf{x}^-,\mathbf{x})u_\gamma(\mathbf{x})d\Gamma = \int_\Gamma U^*_{\alpha\beta\gamma}(\mathbf{x}^-,\mathbf{x})t_\gamma(\mathbf{x})d\Gamma \tag{11}$$

where $\oint$=stands for the Hadamard principal value integral. The plate bending stress resultants boundary integral equation can be written as follows

$$\begin{aligned}&\frac{1}{2}M_{\alpha\beta}(\mathbf{x}^-)+\frac{1}{2}M_{\alpha\beta}(\mathbf{x}^+)+\oint_\Gamma P^*_{\alpha\beta\gamma}(\mathbf{x}^-,\mathbf{x})w_\gamma(\mathbf{x})d\Gamma\\&\quad+\oint_\Gamma P^*_{\alpha\beta3}(\mathbf{x}^-,\mathbf{x})w_3(\mathbf{x})d\Gamma\\&=\int_\Gamma W^*_{\alpha\beta\gamma}(\mathbf{x}^-,\mathbf{x})p_\gamma(\mathbf{x})d\Gamma+\int_\Gamma W^*_{\alpha\beta3}(\mathbf{x}^-,\mathbf{x})p_3(\mathbf{x})d\Gamma\\&\quad+\lambda\int_\Omega W^*_{\alpha\beta3}(\mathbf{x}^-,\mathbf{X})qd\Omega\\&\quad+\lambda\int_\Omega W^*_{\alpha\beta3}(\mathbf{x}^-,\mathbf{X})(N_{\theta\psi,\theta}w_{3,\psi}+N_{\theta\psi}w_{3,\psi\theta})d\Omega\end{aligned} \tag{12}$$

and

$$\begin{aligned}&\frac{1}{2}Q_\beta(\mathbf{x}^-)+\frac{1}{2}Q_\beta(\mathbf{x}^+)+\oint_\Gamma P^*_{3\beta\gamma}(\mathbf{x}^-,\mathbf{x})w_\gamma(\mathbf{x})d\Gamma\\&\quad+\oint_\Gamma P^*_{3\beta3}(\mathbf{x}^-,\mathbf{x})w_3(\mathbf{x})d\Gamma\\&=\int_\Gamma W^*_{3\beta\gamma}(\mathbf{x}^-,\mathbf{x})p_\gamma(\mathbf{x})d\Gamma+\int_\Gamma W^*_{3\beta3}(\mathbf{x}^-,\mathbf{x})p_3(\mathbf{x})d\Gamma\\&\quad+\lambda\int_\Omega W^*_{3\beta3}(\mathbf{x}^-,\mathbf{X})qd\Omega\\&\quad+\lambda\int_\Omega W^*_{3\beta3}(\mathbf{x}^-,\mathbf{X})(N_{\theta\psi,\theta}w_{3,\psi}+N_{\theta\psi}w_{3,\psi\theta})d\Omega\end{aligned} \tag{13}$$

where λ is critical load factor and $U^*_{\alpha\beta\gamma}$, $T^*_{\alpha\beta\gamma}$, $P^*_{\alpha\beta\gamma}$, $P^*_{\alpha\beta3}$, $W^*_{\alpha\beta\gamma}$ and $W^*_{\alpha\beta3}$ are the fundamental solutions and are listed in Appendix A.

Multiplying equations (11-13) by the outward normal $n_\beta(\mathbf{x}^-)$ and denoting that $n_\beta(\mathbf{x}^+)=-n_\beta(\mathbf{x}^-)$, the traction integral equations for a boundary source point at lower crack surface $\mathbf{x}^-$ are as follows:

$$\frac{1}{2}t_\alpha(\mathbf{x}^-)-\frac{1}{2}t_\alpha(\mathbf{x}^+)+n_\beta(\mathbf{x}^-)\oint_\Gamma T^*_{\alpha\beta\gamma}(\mathbf{x}^-,\mathbf{x})u_\gamma(\mathbf{x})d\Gamma = n_\beta(\mathbf{x}^-)\int_\Gamma U^*_{\alpha\beta\gamma}(\mathbf{x}^-,\mathbf{x})t_\gamma(\mathbf{x})d\Gamma \tag{14}$$

and

$$\begin{aligned}&\frac{1}{2}p_\alpha(\mathbf{x}^-)-\frac{1}{2}p_\alpha(\mathbf{x}^+)+n_\beta(\mathbf{x}^-)\oint_\Gamma P^*_{\alpha\beta\gamma}(\mathbf{x}^-,\mathbf{x})w_\gamma(\mathbf{x})d\Gamma\\&+\ n_\beta(\mathbf{x}^-)\oint_\Gamma P^*_{\alpha\beta3}(\mathbf{x}^-,\mathbf{x})w_3(\mathbf{x})d\Gamma\\&=n_\beta(\mathbf{x}^-)\oint_\Gamma W^*_{\alpha\beta\gamma}(\mathbf{x}^-,\mathbf{x})p_\gamma(\mathbf{x})d\Gamma\\&\quad+n_\beta(\mathbf{x}')\int_\Gamma W^*_{\alpha\beta3}(\mathbf{x}^-,\mathbf{x})p_3(\mathbf{x})d\Gamma\\&\quad+\lambda n_\beta(\mathbf{x}^-)\int_\Omega W^*_{\alpha\beta3}(\mathbf{x}^-,\mathbf{X})qd\Omega\\&\quad+\lambda n_\beta(\mathbf{x}^-)\int_\Omega W^*_{\alpha\beta3}(\mathbf{x}^-,\mathbf{X})(N_{\theta\psi,\theta}w_{3,\psi}+N_{\theta\psi}w_{3,\psi\theta})d\Omega\end{aligned} \tag{15}$$

$$\begin{aligned}&\frac{1}{2}p_3(\mathbf{x}^-)-\frac{1}{2}p_3(\mathbf{x}^+)+n_\beta(\mathbf{x}^-)\oint_\Gamma P^*_{3\beta\gamma}(\mathbf{x}^-,\mathbf{x})w_\gamma(\mathbf{x})d\Gamma\\&+n_\beta(\mathbf{x}^-)\oint_\Gamma P^*_{3\beta3}(\mathbf{x}^-,\mathbf{x})w_3(\mathbf{x})d\Gamma\\&=n_\beta(\mathbf{x}^-)\int_\Gamma W^*_{3\beta\gamma}(\mathbf{x}^-,\mathbf{x})p_\gamma(\mathbf{x})d\Gamma\\&\quad+n_\beta(\mathbf{x}^-)\oint_\Gamma W^*_{3\beta3}(\mathbf{x}^-,\mathbf{x})p_3(\mathbf{x})d\Gamma\\&\quad+\lambda n_\beta(\mathbf{x}^-)\int_\Omega W^*_{3\beta3}(\mathbf{x}^-,\mathbf{X})qd\Omega\\&\quad+\lambda n_\beta(\mathbf{x}^-)\int_\Omega W^*_{3\beta3}(\mathbf{x}^-,\mathbf{X})(N_{\theta\psi,\theta}w_{3,\psi}+N_{\theta\psi}w_{3,\psi\theta})d\Omega\end{aligned} \tag{16}$$

To arrange an eigenvalue equation, the derivatives of w_3 have to be expressed in terms of $w_3(\mathbf{X})$. The $w_{3,\beta}(\mathbf{X})$ and $w_{3,\alpha\beta}(\mathbf{X})$ terms are approximated by a radial basis function $f(r)$ as follows;

$$w_3(x_1,x_2)=\sum_{m=1}^{M}f(r)^m\Psi^m \tag{17}$$

where $f(r)=1+r$ is the a radial basis function, and M is the total number of selected points.

$$r=\sqrt{(x_1-x_1^m)^2+(x_2-x_2^m)^2} \tag{18}$$

The Ψ^m are coefficients which are determined by values at the selected points M as follows

$$\mathbf{\Psi}=\mathbf{F}^{-1}\mathbf{w}_3 \tag{19}$$

Therefore, the first derivative of deflection $w_{3,\beta}$ is expressed as

$$w_{3,\beta}(x_1,x_2) = \mathbf{f}(r)_{,\beta}(\mathbf{F}^{-1}\mathbf{w}_3) \tag{20}$$

The second derivative of deflection $w_{3,\alpha\beta}$ can be derived in a similar way as above

$$\mathbf{\Psi} = \mathbf{F}^{-1}\mathbf{w}_{3,\beta} \tag{21}$$

Therefore,

$$w_{3,\alpha\beta}(x_1,x_2) = \mathbf{f}(r)_{,\alpha}(\mathbf{F}^{-1}\mathbf{w}_{3,\beta}) \tag{22}$$

Substituting equation (20) into equation (22), gives:

$$w_{3,\alpha\beta}(x_1,x_2) = \mathbf{f}(r)_{,\alpha}\mathbf{F}^{-1}(\mathbf{f}(r)_{,\beta}\mathbf{F}^{-1}\mathbf{w}_3) \tag{23}$$

Similar to the above expressions, the derivative of in-plane stress resultants $N_{\alpha\beta,\alpha}$ can be expressed as

$$N_{\alpha\beta,\alpha}(x_1,x_2) = \mathbf{f}(r)_{,\alpha}\mathbf{F}^{-1}N_{\alpha\beta}^{linear} \tag{24}$$

The equation (8) can be expressed as

$$\begin{aligned}&\frac{1}{2}w_j(\mathbf{x}^+)+\frac{1}{2}w_j(\mathbf{x}^-)+\int_\Gamma P_{ij}^*(\mathbf{x}^+,\mathbf{x})w_j(\mathbf{x})\,d\Gamma\\ &\quad=\int_\Gamma W_{ij}^*(\mathbf{x}^+,\mathbf{x})p_j(\mathbf{x})\,d\Gamma\\ &\quad+\lambda\int_\Omega W_{i3}^*(\mathbf{x}^+,\mathbf{X})f_b(\mathbf{X})d\Omega\end{aligned} \tag{25}$$

where

$$\begin{aligned}f_b &= q+N_{\alpha\beta,\alpha}\mathbf{f}(r)_{,\beta}\mathbf{F}^{-1}w_3\\ &\quad+N_{\alpha\beta}\mathbf{f}(r)_{,\alpha}\mathbf{F}^{-1}\mathbf{f}(r)_{,\beta}\mathbf{F}^{-1}w_3\end{aligned} \tag{26}$$

The equations (12) and (13) are written as

$$\begin{aligned}&\frac{1}{2}M_{\alpha\beta}(\mathbf{x}^-)+\frac{1}{2}M_{\alpha\beta}(\mathbf{x}^+)+\oint_\Gamma P_{\alpha\beta\gamma}^*(\mathbf{x}^-,\mathbf{x})w_\gamma(\mathbf{x})d\Gamma\\ &+\oint_\Gamma P_{\alpha\beta3}^*(\mathbf{x}^-,\mathbf{x})w_3(\mathbf{x})d\Gamma\\ &=\oint_\Gamma W_{\alpha\beta\gamma}^*(\mathbf{x}^-,\mathbf{x})p_\gamma(\mathbf{x})d\Gamma(\mathbf{x})+\int_\Gamma W_{\alpha\beta3}^*(\mathbf{x}^-,\mathbf{x})p_3(\mathbf{x})d\Gamma\\ &\quad+\lambda\int_\Omega W_{\alpha\beta3}^*(\mathbf{x}^-,\mathbf{X})f_b d\Omega\end{aligned} \tag{27}$$

and

$$\begin{aligned}&\frac{1}{2}Q_\beta(\mathbf{x}^-)+\frac{1}{2}Q_\beta(\mathbf{x}^+)+\int_\Gamma P_{3\beta\gamma}^*(\mathbf{x}^-,\mathbf{x})w_\gamma(\mathbf{x})d\Gamma\\ &+\oint_\Gamma P_{3\beta3}^*(\mathbf{x}^-,\mathbf{x})w_3(\mathbf{x})d\Gamma\\ &=\int_\Gamma W_{3\beta\gamma}^*(\mathbf{x}^-,\mathbf{x})p_\gamma(\mathbf{x})d\Gamma(\mathbf{x})+\int_\Gamma W_{3\beta3}^*(\mathbf{x}^-,\mathbf{x})p_3(\mathbf{x})d\Gamma\\ &\quad+\lambda\int_\Omega W_{3\beta3}^*(\mathbf{x}^-,\mathbf{X})f_b d\Omega\end{aligned} \tag{28}$$

The traction boundary integral equations (15) and (16) are written as

$$\begin{aligned}&\frac{1}{2}p_\alpha(\mathbf{x}^-)-\frac{1}{2}p_\alpha(\mathbf{x}^+)+n_\beta(\mathbf{x}^-)\oint_\Gamma P_{\alpha\beta\gamma}^*(\mathbf{x}^-,\mathbf{x})w_\gamma(\mathbf{x})d\Gamma\\ &+n_\beta(\mathbf{x}^-)\oint_\Gamma P_{\alpha\beta3}^*(\mathbf{x}^-,\mathbf{x})w_3(\mathbf{x})d\Gamma\\ &=n_\beta(\mathbf{x}^-)\oint_\Gamma W_{\alpha\beta\gamma}^*(\mathbf{x}^-,\mathbf{x})p_\gamma(\mathbf{x})d\Gamma\\ &\quad+n_\beta(\mathbf{x}')\int_\Gamma W_{\alpha\beta3}^*(\mathbf{x}^-,\mathbf{x})p_3(\mathbf{x})d\Gamma\\ &\quad+\lambda n_\beta(\mathbf{x}^-)\int_\Omega W_{\alpha\beta3}^*(\mathbf{x}^-,\mathbf{X})f_b d\Omega\end{aligned} \tag{29}$$

$$\begin{aligned}&\frac{1}{2}p_3(\mathbf{x}^-)-\frac{1}{2}p_3(\mathbf{x}^+)+n_\beta(\mathbf{x}^-)\int_\Gamma P_{3\beta\gamma}^*(\mathbf{x}^-,\mathbf{x})w_\gamma(\mathbf{x})d\Gamma\\ &+n_\beta(\mathbf{x}^-)\oint_\Gamma P_{3\beta3}^*(\mathbf{x}^-,\mathbf{x})w_3(\mathbf{x})d\Gamma\\ &=n_\beta(\mathbf{x}^-)\int_\Gamma W_{3\beta\gamma}^*(\mathbf{x}^-,\mathbf{x})p_\gamma(\mathbf{x})d\Gamma\\ &\quad+n_\beta(\mathbf{x}^-)\oint_\Gamma W_{3\beta3}^*(\mathbf{x}^-,\mathbf{x})p_3(\mathbf{x})d\Gamma\\ &\quad+\lambda n_\beta(\mathbf{x}^-)\int_\Omega W_{3\beta3}^*(\mathbf{x}^-,\mathbf{X})f_b d\Omega\end{aligned} \tag{30}$$

The deflection equation w_3 at the domain points $\mathbf{X}'$ can be written as follows

$$\begin{aligned}w_3(\mathbf{X}') &= \int_\Gamma W_{3j}^*(\mathbf{X}',x)p_j(x)d\Gamma\\ &\quad-\int_\Gamma P_{3j}^*(\mathbf{X}',x)w_j(x)d\Gamma\\ &\quad+\lambda\int_\Omega W_{33}^*(\mathbf{X}',\mathbf{X})f_b(\mathbf{X})\,d\Omega\end{aligned} \tag{31}$$

Equations (7) and (8) and (14, 29, 30) represent displacement and traction integral equations respectively on the

crack surfaces, and together with the use of the displacement integral equations as follows

$$c_{\theta\alpha}\left(\mathbf{x}'\right)u_\alpha(\mathbf{x}')+\int_\Gamma T^*_{\theta\alpha}(\mathbf{x}',\mathbf{x})u_\alpha(\mathbf{x})d\Gamma = \int_\Gamma U^*_{\theta\alpha}(\mathbf{x}',\mathbf{x})t_\alpha(\mathbf{x})d\Gamma \tag{32}$$

and

$$c_{ij}(\mathbf{x}')w_j(\mathbf{x}')+\int_\Gamma P^*_{ij}(\mathbf{x}',\mathbf{x})w_j(\mathbf{x})\,d\Gamma = \int_\Gamma W^*_{ij}(\mathbf{x}',\mathbf{x})p_j(\mathbf{x})\,d\Gamma + \lambda\int_\Omega W^*_{i3}(\mathbf{x}',\mathbf{X})f_b(\mathbf{X})d\Omega \tag{33}$$

for collocation points on the rest of the boundary Γ_b (see Figure 1), form the dual boundary integral formulation.

4 Transformation of The Domain Integrals

The dual reciprocity method for shear deformable plate developed by [Wen, Aliabadi and Young (2000)] can be used to evaluate the domain integrals appearing in the dual boundary integral equation formulation. Assume that the term f_b are the body forces, therefore they can be approximated by

$$f_b=\sum_{m=1}^{M} f(r)^m\phi^m \tag{34}$$

where $f(r)$ is a radial basis function (see Appendix), the ϕ^m_j are a set of unknown coefficients, r is denoted as the equation (18), M is the total number of the selected points.

The ϕ^m_j are coefficients which are determined by values at the selected points M as follows

$$\phi=\mathbf{F}^{-1}\mathbf{f}_b \tag{35}$$

As the source point $\mathbf{x}^+\in\Gamma^+$ is coincident with $\mathbf{x}^-\in\Gamma^-$, it is important to note when the dual reciprocity technique is applied to a structure containing cracks, domain integrals will contain extra free terms as in equations (25-28).

The domain integral in equation (25) is rewritten as:

$$\begin{aligned}&\int_\Omega W^*_{i3}(x',X)f_b(X)d\Omega\\ &=\sum_{m=1}^{M}\Big[\frac{1}{2}\hat{w}_{mj}(x^+)+\frac{1}{2}\hat{w}_{mj}(x^-)\\ &\quad+\int_\Gamma P^*_{ij}(x',x)\hat{w}_{mj}(x)d\Gamma\\ &\quad-\int_\Gamma W^*_{ij}(x',x)\hat{p}_{mj}(x)d\Gamma\Big]\mathbf{F}^{-1}f_b\end{aligned} \tag{36}$$

The domain integral in equation (27) is rewritten as:

$$\begin{aligned}&\int_\Omega W^*_{\alpha\beta3}(\mathbf{x}^-,\mathbf{X})f_{b2}(X)d\Omega\\ &=\{\sum_{m=1}^{M}\Big[\frac{1}{2}\hat{M}_{m\alpha\beta}(\mathbf{x}^-)+\frac{1}{2}\hat{M}_{m\alpha\beta}(\mathbf{x}^+)\\ &\quad+\int_\Gamma P^*_{\alpha\beta\gamma}(\mathbf{x}^-,\mathbf{x})\hat{w}_{m\gamma}(\mathbf{x})d\Gamma\\ &\quad+\int_\Gamma P^*_{\alpha\beta3}(\mathbf{x}^-,\mathbf{x})\hat{w}_{m3}(\mathbf{x})d\Gamma\\ &\quad-\int_\Gamma W^*_{\alpha\beta\gamma}(\mathbf{x}^-,\mathbf{x})\hat{p}_{m\gamma}(\mathbf{x})d\Gamma\\ &\quad-\int_\Gamma W^*_{\alpha\beta3}(\mathbf{x}^-,\mathbf{x})\hat{p}_{m3}(\mathbf{x})d\Gamma\Big](\mathbf{F}^{-1}\mathbf{f}_b)^m\}\end{aligned} \tag{37}$$

The domain integral in equation (28) is rewritten as:

$$\begin{aligned}&\int_\Omega W^*_{3\beta3}(\mathbf{x}^-,\mathbf{X})f_{b2}(X)d\Omega\\ &=\{\sum_{m=1}^{M}\Big[\frac{1}{2}\hat{Q}_{m\beta}(\mathbf{x}^-)+\frac{1}{2}\hat{Q}_{m\beta}(\mathbf{x}^+)\\ &\quad+\int_\Gamma P^*_{3\beta\gamma}(\mathbf{x}^-,\mathbf{x})\hat{w}_{m\gamma}(\mathbf{x})d\Gamma\\ &\quad+\int_\Gamma P^*_{3\beta3}(\mathbf{x}^-,\mathbf{x})\hat{w}_{m3}(\mathbf{x})d\Gamma\\ &\quad-\int_\Gamma W^*_{3\beta\gamma}(\mathbf{x}^-,\mathbf{x})\hat{p}_{m\gamma}(\mathbf{x})d\Gamma\\ &\quad-\int_\Gamma W^*_{3\beta3}(\mathbf{x}^-,\mathbf{x})\hat{p}_{m3}(\mathbf{x})d\Gamma\Big](\mathbf{F}^{-1}\mathbf{f}_b)^m\}\end{aligned} \tag{38}$$

An alternative method for transformation of domain integrals to boundary ones has recently been proposed [Ochiai and Sladek (2004)].

5 Numerical Implementation

Crack modelling strategy, special crack-tip elements, crack modelling consideration of the dual reciprocity technique, treatment of the singularities used in this work

are similar with those described in [Dirgantara and Aliabadi (2000)] which follow the general guidelines originally reported in [Portela and Aliabadi (1992), Mi and Aliabadi (1992)]. They can be summarized as follows:

- crack surfaces are discretized with discontinuous quadratic elements to satisfy continuity conditions of displacements and its derivatives on all nodes for the existence of principal value integrals;
- the traction equations are applied for collocation on one of the crack surfaces;
- the displacement equations are applied for collocation on the opposite crack surface and other non-crack boundaries;
- continuous quadratic elements are applied along the remaining boundary of the body, except at the intersection between a crack and an edge, where discontinuous or semi-discontinuous elements are required on the edge in order to avoid a common node at intersection, and also at boundary corner, where semi-discontinuous elements are used in order to avoid a common node at the corner;
- special crack tip discontinuous elements to accurately represent the $\sqrt{r}$ behaviour of the displacement field are used [see Aliabadi (2002)].

6 Numerical Implementation

The numerical implementation of the dual boundary element method for buckling analysis of cracked plated is presented in this section. The first step is to solve the dual boundary integrals of in-plane problem and then calculate the stress resultants at the domain points. The second step is to solve the dual boundary integral formulation for buckling problems.

6.1 Determination of the in-plane stresses

After discretizing the boundaries and introducing boundary conditions into equations (32), (7) and (14), the system of algebraic equation can be arranged in terms of the known and unknown quantities as follows:

$$[\mathbf{A}]\{\mathbf{X}\} = \{\mathbf{F}\} \tag{39}$$

where matrix $\mathbf{X}$ contains the unknown vectors of displacements $\mathbf{u}$ and tractions $\mathbf{t}$. The vector $\mathbf{F}$ is obtained by multiplying the related coefficient matrices by the known vectors of displacements $\mathbf{u}$ or tractions $\mathbf{t}$.

Once equation (39) has been solved, in-plane stresses N_{11}, N_{12}, and N_{22} in the domain (equation (9)) can be calculated. The stresses are required to solve the cracked plate buckling problem.

6.2 Solving the plate buckling problem

After applying the boundary conditions to equations (33), (25), (29) and (30), they can be written in a matrix form as:

$$[\mathbf{C}]\{\mathbf{w}\} + [\mathbf{H}^p]\{\mathbf{w}\} = [\mathbf{G}^p]\{\mathbf{p}\} + \lambda[\mathbf{G}^p_{eq}]\{\mathbf{f}_b\} \tag{40}$$

in which $\mathbf{H}^p$ and $\mathbf{G}^p$ are boundary element influence matrices for plate bending, $\hat{\mathbf{w}}$ and $\hat{\mathbf{p}}$ are matrices of node values of particular solution on the boundary and $\mathbf{G}^p_{eq} = (\mathbf{H}^p\hat{\mathbf{w}} - \mathbf{G}^p\hat{\mathbf{p}})\mathbf{F}^{-1}$. The $q(\mathbf{X})$ quantities are initialized to zero and the term $f_b(\mathbf{X})$ is expressed in term of $w_3(\mathbf{X})$, as follows

$$f_b(\mathbf{X}) = \mathbf{f}_{bw}(\mathbf{X})w_3(\mathbf{X}) \tag{41}$$

where $\mathbf{f}_{bw} = N_{\alpha\beta,\alpha}\mathbf{f}(r)_{,\beta}\mathbf{F}^{-1} + N_{\alpha\beta}\mathbf{f}(r)_{,\alpha}\mathbf{F}^{-1}(\mathbf{f}(r)_{,\beta}\mathbf{F}^{-1})$

Equation (40) can be arranged in a similar manner as equation (39), and give

$$[\mathbf{B}]_{3N\times 3N}\{\mathbf{Y}\}_{3N} = \lambda[\mathbf{K}]_{3N\times L}\{\mathbf{w}_3\}_L \tag{42}$$

$$\mathbf{K} = \mathbf{G}^p_{eq}\mathbf{f}_{bw} \tag{43}$$

where the matrix $\mathbf{B}$ contains the coefficient matrices $\mathbf{H}^p$ and $\mathbf{G}^p$. N and L are the number of boundary elements and domain points, respectively.

The equation (31) can be also written in matrix form as follows:

$$[\mathbf{I}]\{\mathbf{w}_3\}_L = [\mathbf{BB}]_{L\times 3N}\{\mathbf{Y}\}_{3N} + \lambda[\mathbf{KK}]_{L\times L}\{\mathbf{w}_3\}_L \tag{44}$$

where matrix $[\mathbf{I}]$ is an identity matrix. The matrix $[\mathbf{BB}]$ contains coefficient matrices related to fundamental solutions. The matrix $[\mathbf{KK}]$ are obtained by multiplication of coefficient matrices related to the fundamental solutions with matrix $\mathbf{f}_{bw}$.

The equation (42) can be rearranged in term of unknown vector $\{\mathbf{Y}\}_{3N}$,

$$\{\mathbf{Y}\}_{3N} = \lambda[\mathbf{B}]^{-1}_{3N\times 3N}[\mathbf{K}]_{3N\times L}\{\mathbf{w}_3\}_L \tag{45}$$

where matrix $\mathbf{B}^{-1}$ is the inverse matrix of $\mathbf{B}$.

The substitution of the equation (45) into the equation (44) yields:

$$[\mathbf{I}]\{\mathbf{w}_3\}_L = \lambda[\mathbf{BB}]_{L\times 3N}[\mathbf{B}]^{-1}_{3N\times 3N}[\mathbf{K}]_{3N\times L}\{\mathbf{w}_3\}_L + \lambda[\mathbf{KK}]_{L\times L}\{\mathbf{w}_3\}_L \quad (46)$$

Then,

$$[\mathbf{I}]\{\mathbf{w}_3\}_L = \lambda([\mathbf{BB}]_{L\times 3N}[\mathbf{B}]^{-1}_{3N\times 3N}[\mathbf{K}]_{3N\times L} + [\mathbf{KK}]_{L\times L})\{\mathbf{w}_3\}_L \quad (47)$$

The equation (47) can be written as a standard eigenvalue problem equation as follows:

$$([\psi] - \frac{1}{\lambda}[\mathbf{I}])\{\mathbf{w}_3\}_L = 0 \quad (48)$$

where $[\psi] = [\mathbf{BB}]_{L\times 3N}[\mathbf{B}]^{-1}_{3N\times 3N}[\mathbf{K}]_{3N\times L} + [\mathbf{KK}]_{L\times L}$.
Analysis of shear deformable cracked plate buckling problems has been presented as a standard eigenvalue problem. Buckling coefficients correspond to the problem can be obtained by the solution of equation (48).

7 Numerical Examples

Several numerical examples are presented to demonstrate the accuracy of the proposed method for analysis of plate buckling problems with different geometries and boundary conditions. The calculated values of K are compared with analytical [Stahl and Keer (1972)] and differential quadrature element method [Liu (2001)] results. In the following examples, the buckling coefficient K is defined by

$$K = \frac{b^2}{h^2 E}\sigma_{cr}$$

where σ_{cr} is critical compression load, b is the width of plate.

7.1 Convergence study of simply supported rectangular cracked plates subjected to compression loads

In this example, convergence of the proposed formulation is assessed by solving a simply supported cracked plates as shown in Figure 2. Two configurations of rectangular plate with aspect ratio $a/b = 2$ are considered here: (i) a longitudinal central crack with $2c/a = 0.25$ and (ii) a transverse central crack with $2c/b = 0.25$. Both models are discretized into 8 elements on the long sides and 4 elements on the short sides. Each model has different meshes on the crack surfaces. The BEM results are shown in Figure 3. As it can be seen, buckling coefficients for model (i) in Figure 2 are not sensitive to the number of elements on the crack surfaces and convergence is achieved with only 8 elements on the crack surfaces. The convergence for model (ii) can be achieved with as few as 14 elements on the crack surfaces.

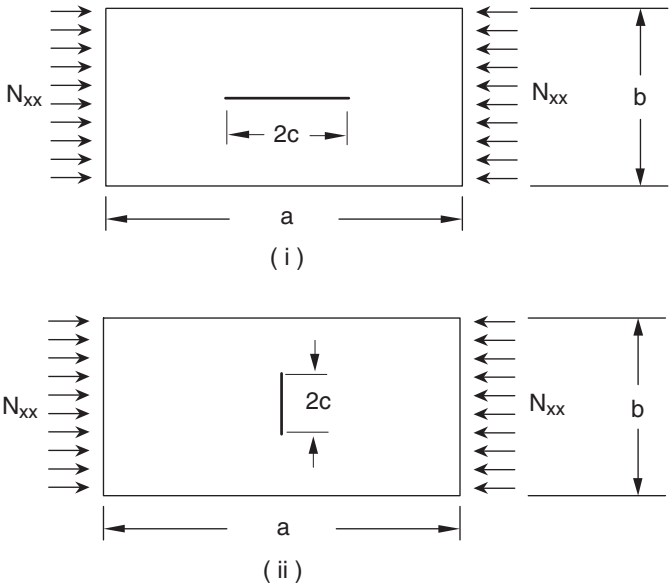

Figure 2 : Rectangular plates with a central crack subjected to compression loads.

7.2 Simply supported rectangular plates with a longitudinal central crack

Here, the problem of the rectangular plate with a longitudinal central crack subjected to compression load is studied again. The model is similar to that shown in Figure 2 (i) but the aspect ratio of the plate are varied. Two configurations are considered: (a) the plate with aspect ratio $a/b = 1$ and (b) the plate with aspect ratio $a/b = 2$. [Stahl and Keer (1972)] have analysed the first case. Both cases were analysed by [Liu (2001)]. Buckling coefficients for different aspect ratios of crack length to the length of plate $2c/a$ are presented in Figures 4 and 5. Figures 6 and 7 present the change in the buckling modes of rectangular plate with aspect ratio $a/b = 2$. For the case of short cracks (aspect ratio $2c/a$ up to 0.25), the buckling modes are illustrated in Figure 6. When the aspect ratio $2c/a$ is greater than 0.25, the buckling modes change as shown in Figure 7. It can be seen from the Fig-

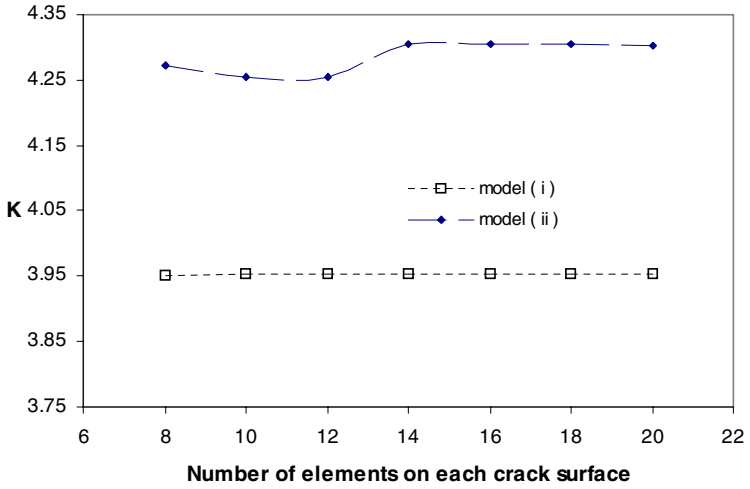

Figure 3 : Convergence study for the problem of cracked plates buckling.

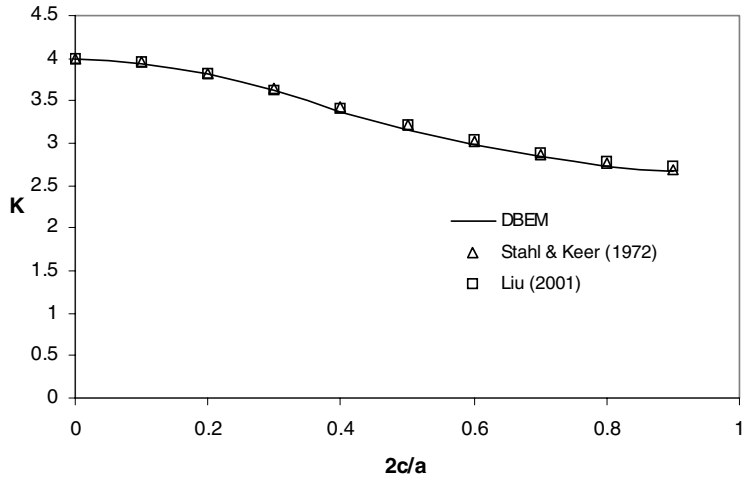

Figure 4 : Variation of buckling coefficients for the plate (aspect ratio $a/b = 1$) with a longitudinal central crack.

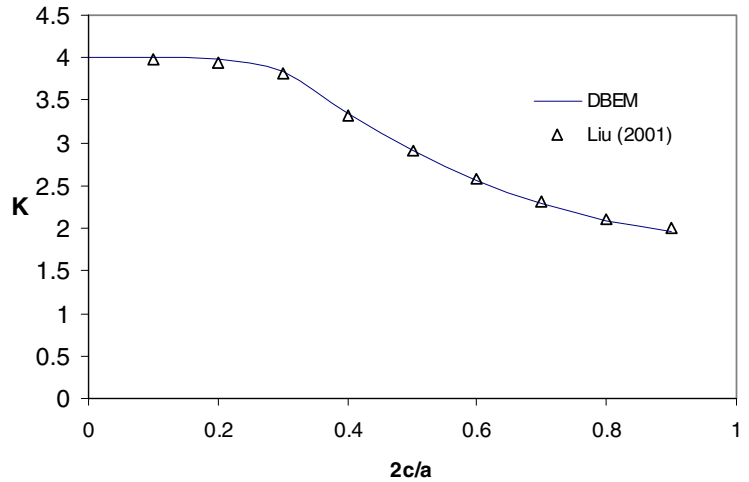

Figure 5 : Variation of buckling coefficients for the plate (aspect ratio $a/b = 2$) with a longitudinal central crack.

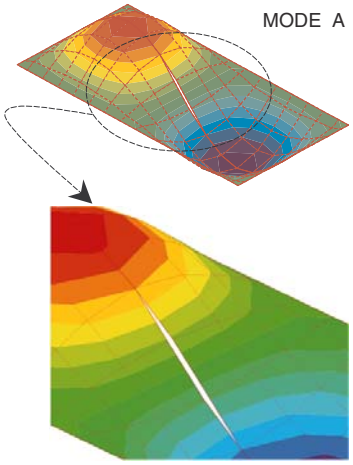

Figure 6 : Mode A: initial mode of simply supported rectangular plate with a longitudinal central crack.

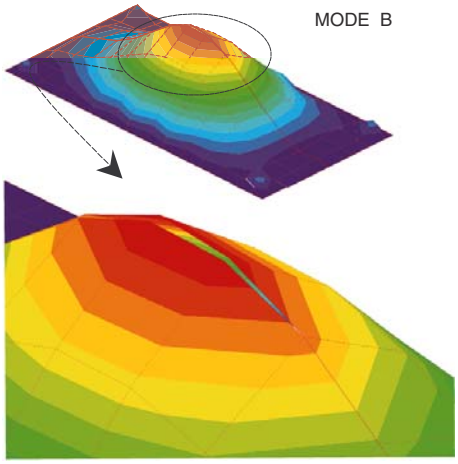

Figure 7 : Mode B: second mode of simply supported rectangular plate with a longitudinal central crack.

ures that the present results are in very good agreements (less than 1% difference) with those presented in [Stahl and Keer (1972) and Liu (2001)].

7.3 Simply supported rectangular plates with a longitudinal edge crack

In this example, a rectangular plate with a longitudinal edge crack subjected to compression loads is studied. The model is shown in Figure 8. Two configurations of the edge crack plate are considered: (a) aspect ratio $a/b = 1$ and (b) aspect ratio $a/b = 2$. The second case has been analysed by [Stahl and Keer (1972), and Liu (2001)] has investigated both cases. Buckling coefficients for different aspect ratios of crack length to the length of plate c/a are presented in Figures 9 and 10. It can be seen from the Figures that good agreements (less than 1.5% difference) are achieved with those presented in [Stahl and Keer (1972) and Liu (2001)].

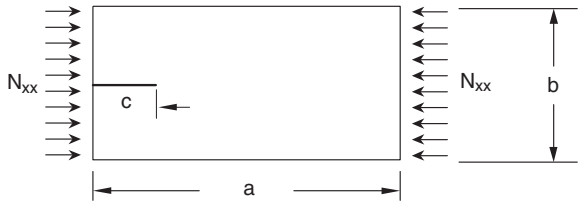

Figure 8 : Rectangular plate with a longitudinal edge crack.

7.4 Rectangular plates with a longitudinal central crack and different boundary conditions

A rectangular plate with a longitudinal central crack subjected to compression loads with different boundary conditions is presented. The model is similar to that shown in Figure 2 (i) with aspect ratio of the plate $a/b = 2$. Buckling coefficients for different aspect ratios of crack length to the length of plate $2c/a$ are presented in Figure 11. The legends in the Figure 11 are defined as:

cccc	:	sides and ends clamped
ssss	:	sides and ends simply supported
cscs	:	ends clamped, sides simply supported
scsc	:	sides clamped, ends simply supported

As it can be seen, the buckling coefficients decrease with increasing $2c/a$ for all four different boundary conditions. The buckling coefficient is the highest for cccc and the lowest for ssss.

7.5 Rectangular plates with a longitudinal edge crack and different boundary conditions

Here, a rectangular plate with a longitudinal edge crack subjected to compression loads with different boundary conditions is analysed. The model is similar to that shown in Figure 8 with aspect ratio of the plate $a/b = 2$. Buckling coefficients for different aspect ratios of crack length to the length of plate c/a are presented in Figure 12. The buckling coefficients are shown to decrease with increasing crack length to width ratio.

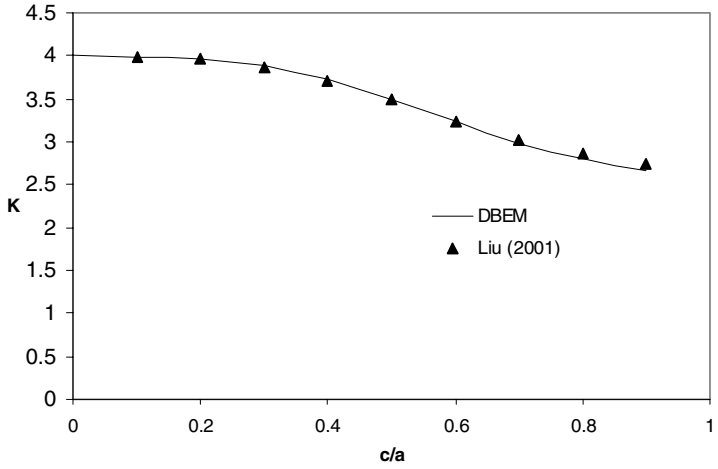

Figure 9 : Variation of buckling coefficients for the plate (aspect ratio $a/b = 1$) with edge crack.

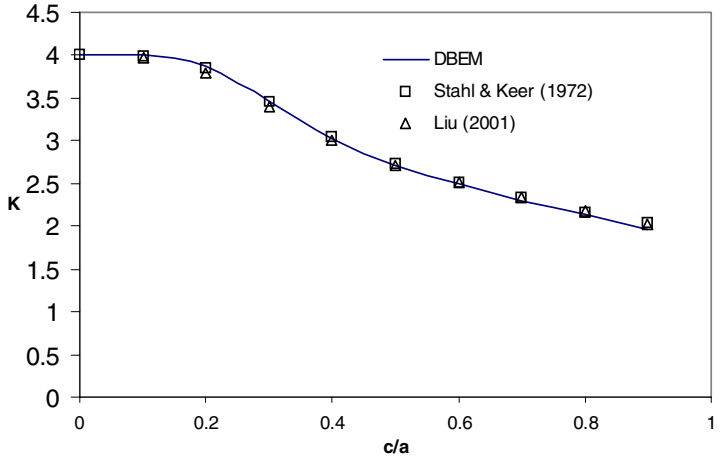

Figure 10 : Variation of buckling coefficients for the plate (aspect ratio $a/b = 2$) with edge crack.

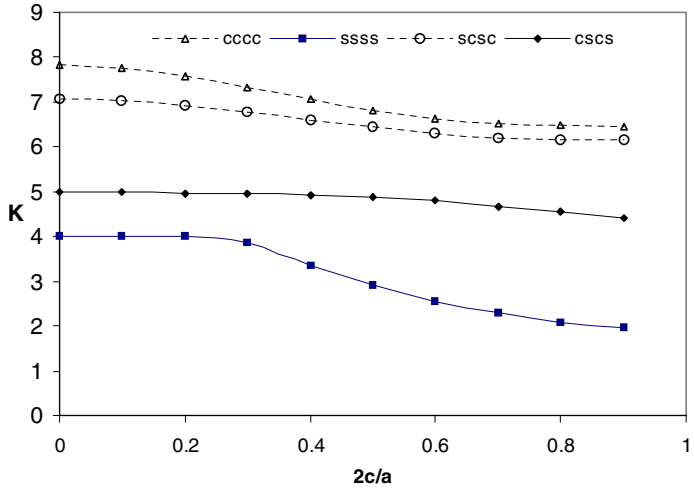

Figure 11 : Variation of buckling coefficients for the plate (aspect ratio $a/b = 2$) with a longitudinal central crack and different boundary conditions.

7.6 Rectangular plate with two collinear cracks

In this example, a rectangular plate with two collinear cracks subjected to compression load with different boundary conditions is analysed. The model is shown in Figure 13 with aspect ratio of the plate $a/b = 2$. Buckling coefficients for different aspect ratios of crack length to the length of plate $2c/a$ and $2e = 0.5a$ are presented in Figure 14. The buckling coefficients for ssss boundary conditions are almost half of those obtained for cccc.

7.7 Rectangular plates with a transverse edge crack

In this example, a rectangular plate with a transverse edge crack as shown in Figure 15 subjected to compression loads is analysed. Aspect ratio of the plate is $a/b = 2$. Two boundary conditions are applied: (a) all sides simply supported (ssss) and (b) one side is clamped and the other side and both ends are simply supported (sssc). Buckling coefficients in different aspect ratios of crack length to the length of plate c/b are presented in Figure 16. As expected the values of K for ssss boundary conditions are lower than cccc.

7.8 Simply supported rectangular plates with a transverse central crack

In this example, a simply supported rectangular plate with a transverse central crack subjected to compression loads is analysed. The model is similar to that shown in Figure 2 (ii) with aspect ratio of the plate $a/b = 2$. Buckling coefficients for different aspect ratios of crack length to the length of plate c/b are presented in Figure 17. Mode A in Figure 17 denotes initial modes for the case of a short crack ($c/b = 0.0$ to $c/b = 0.25$) as shown in Figure 18. It can be seen from Figure 17, as the crack length reaches ratio c/b between $0.25 - 0.275$, the buckling coefficient has a big jump. After the crack length reaches ratio $c/b = 0.275$, the buckling modes change as shown in Figure 19. This phenomena occurs due to the change of buckling mode.

Conclusions

In this paper, the dual boundary element formulation for buckling analysis of shear deformable plates was presented. The traction integral equations were applied on one of the crack surface, while the displacement integral equations were applied on the other crack surface and on all non-crack boundaries to allow for single region modelling of cracked plates.

Discontinuous elements were used to discretize crack surfaces, while continuous elements were used to model all non-crack boundaries, except for corner boundaries and the intersection between a crack and an edge, where semi-discontinuous elements were used. The plate buckling equations were presented as a standard eigenvalue problem. The eigenvalue problem of the plate yields the critical buckling load factor and buckling modes.

Several examples of cracked plates buckling with different geometries and boundary conditions were presented. The BEM results presented were shown to be in good agreements with analytical and other numerical results.

References

Abramowitz, M.; Stegun, I. A. (1965) *Handbook of mathematical functions*, Dover, New York.

Ahmadi-Brooghani, S. Y.; Wearing, J. L. (1996) The application of the dual boundary element method in linear elastic crack problem in plate bending. in *Boundary Element Methods XVIII*, C. A. Brebbia, J. B. Martins, M. H. Aliabadi and N. Haie (Eds.), Portugal, pp. 429-438, Computational Mechanics Publications.

Aliabadi, M. H., (1997a) Boundary element formulations in fracture mechanics, *Applied Mechanics Review*, vol. 50, no. 2, pp. 83-96.

Aliabadi, M. H., (1997b) A new generation of boundary element methods in fracture mechanics, *International Journal of Fracture*, vol. 86, pp. 91-125.

Aliabadi, M. H., (2002) The boundary element method. vol. 2, Applications in solids and structures, Chichester; New York : Wiley.

Dirgantara, T.; Aliabadi, M. H., (2000) Crack growth analysis of plate loaded by bending and tension using dual boundary element method, *International Journal of Fracture*, vol. 105, pp. 27-47.

Dirgantara, T.; Aliabadi, M. H., (2001) *Dual boundary formulation for fracture mechanics analysis of shear deformable shells,* International Journal of Solids Structures, vol. 38 , pp. 7769-7800.

Liu, F.L., (2001) *Differential Quadrature Element Method for Buckling Analysis of Rectangular Mindlin Plates Having Discontinuities,* Int. J. Solids Structures, vol. 38, pp. 2305-2321.

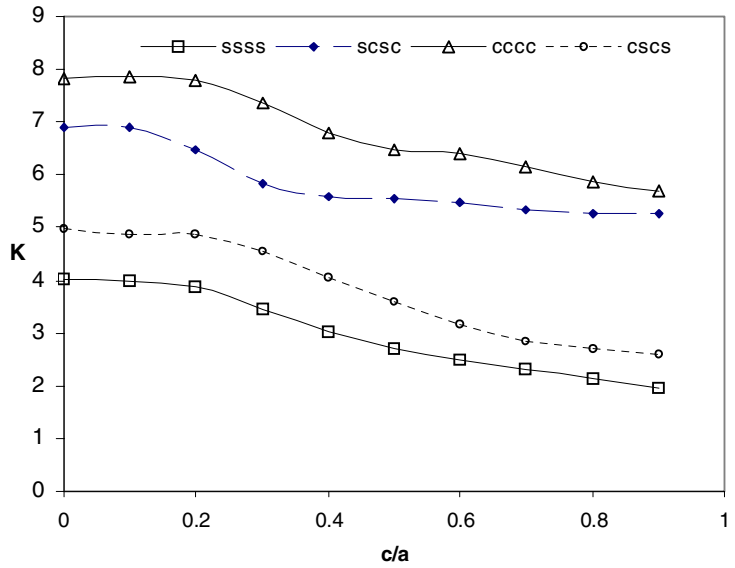

Figure 12 : Rectangular plates $a/b = 2$ with a longitudinal edge crack and different boundary conditions.

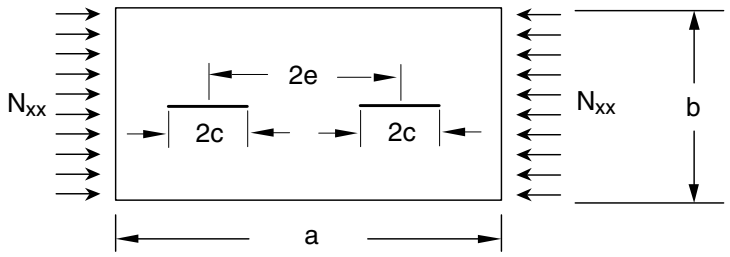

Figure 13 : Rectangular plate with two collinear cracks.

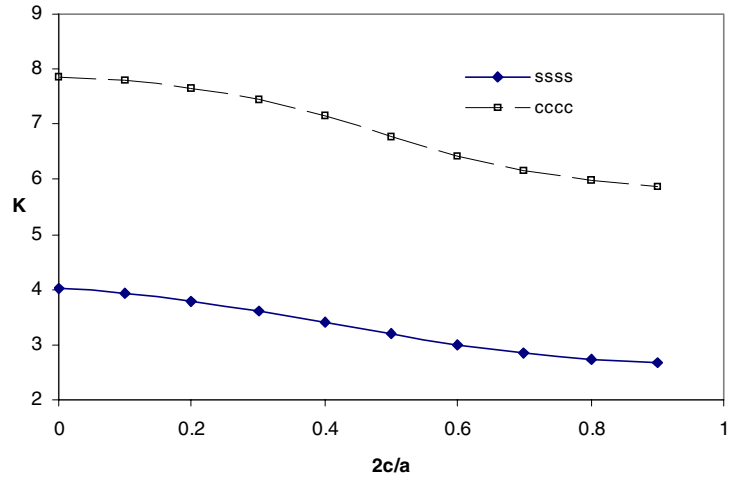

Figure 14 : Variation of buckling coefficients for simply supported plate (aspect ratio $a/b = 2$) with two collinear cracks.

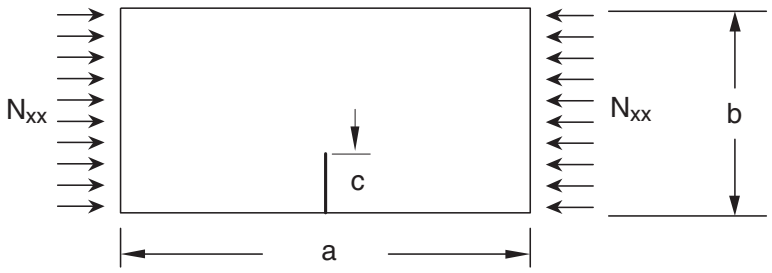

Figure 15 : Rectangular plate with a transverse edge crack.

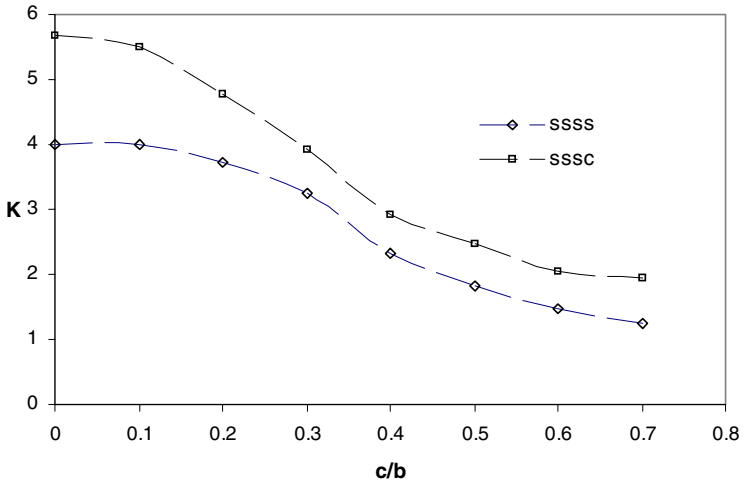

Figure 16 : Variation of buckling coefficients for rectangular plate (aspect ratio $a/b = 2$) with a transverse edge crack.

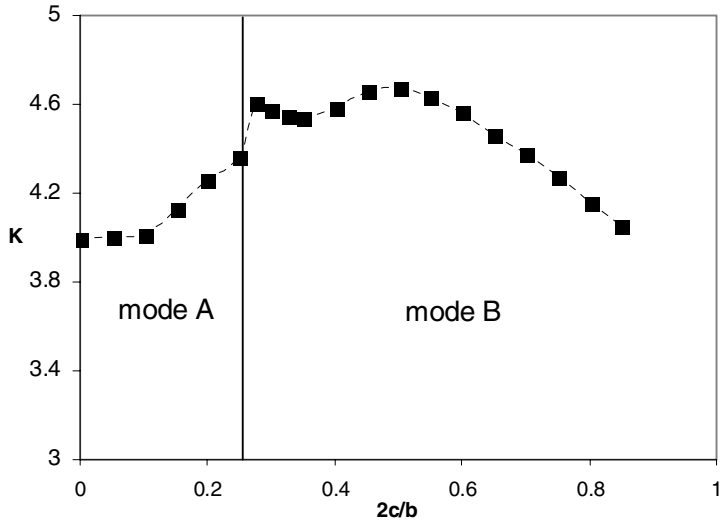

Figure 17 : Rectangular plates with a transverse central crack subjected to compression loads.

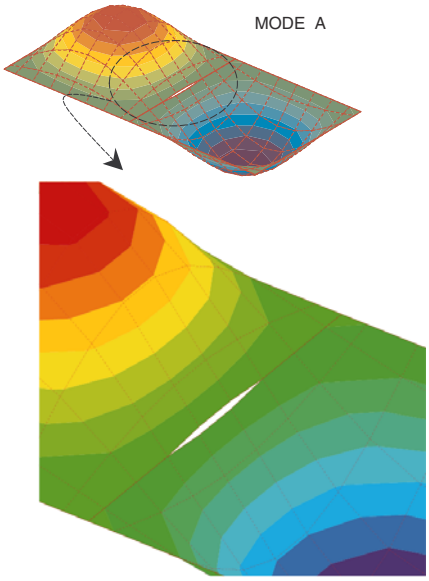

Figure 18 : Mode A: an initial mode of simply supported rectangular plate with a transverse central crack.

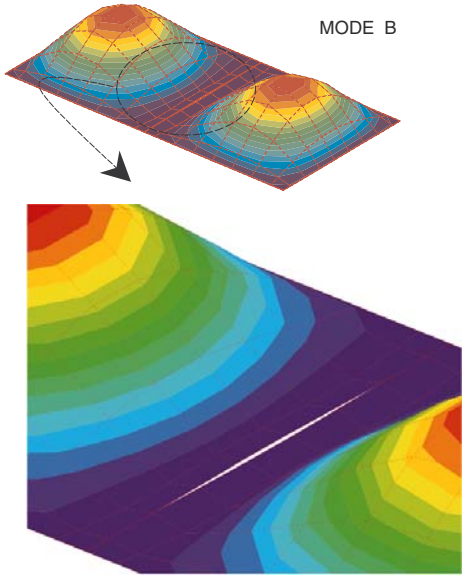

Figure 19 : Mode B: second mode of simply supported rectangular plate with a transverse central crack.

Mi, Y.; Aliabadi, M.H. (1992) Dual boundary element method for three-dimensional fracture mechanics analysis, *Engineering analysis with Boundary Elements,* vol. 10, pp. 161-171.

Nerantzaki, M.S.; Katsikadelis, J.T. (1996) Buckling of plates with variable thickness - an analog equation solution. *Engineering Analysis with Boundary Elements,* vol.18, pp. 149-154.

O.Chiai,Y; Sladek,V. (2004) Numerical treatment of domain integrals without internal cells in three-dimensional BIEM formulations, *CMES: Computer Modeling in Engineering & Sciences,* vol. 6, pp. 525-536.

O'Donoghue, P.E.; Atluri, S.N., (1987) Field/Boundary element approach to the large deflections of thin plates, *Computers and Structures,* vol. 27, pp. 427-436.

Portela, A; Aliabadi, M.H. (1992) The dual boundary element method: efficient implementation for cracked problems, *International Journal for Numerical Methods in Engineering*, vol. 33, pp. 1269-1287.

Purbolaksono, J; Aliabadi, M.H., (2005) Buckling analysis of shear deformable plates by boundary element method, *International Journal for Numerical Methods in Engineering*, vol. 62, pp. 537-563.

Stahl, B.; Keer, L.M., (1972) *Vibration and Stability of Cracked Rectangular Plates,* Int. J. Solids Structures, vol. 8, pp. 69-91.

Syngellakis, S; Elzien,A. (1994) Plate buckling load by the boundary element method, *International Journal for Numerical Methods in Engineering,* vol. 37, pp. 1763-1778.

Vafai, A.; Estekanchi, H.E., (2002) *Parametric Instability of Edge Cracked Plates,* Thin Walled Structures. vol. 40, pp. 29-44

Wen, P. H.; Aliabadi, M. H.; Young, A., (2000) Application of dual reciprocity method to plates and shells, *Engineering Analysis with Boundary Element*, no. 24, pp. 583-590.

Wen, P. H.; Aliabadi, M. H.; Young, A., (2000) Stiffened cracked plates analysis by dual reciprocity method, *International Journal of Fracture*, vol. 106, pp. 245-258.

Vander Weeën, F., (1982) Application of the boundary integral equation method to Reissner's plate model, *International Journal for Numerical Methods in Engineering*, vol. 18, pp. 1-10.

Zhang, J.D.; Atluri,S.N., (1988) Post-buckling analysis of shallow shells by the field-boundary-element method, *International Journal for Numerical Methods in Engineering,* vol. 26, pp. 571-587.

Appendix A: Fundamental Solutions

Appendix A:.1 Plate Bending Problem

The expressions for the kernels W^*_{ij} and P^*_{ij} are given by [Vander Weeën (1982)] as follows:

$$\begin{aligned}
W^*_{\alpha\beta} &= \frac{1}{8\pi D(1-\nu)}\{[8B(z)-(1-\nu)(2\ln z-1)]\delta_{\alpha\beta} \\
&\quad -[8A(z)+2(1-\nu)]r_{,\alpha}r_{,\beta}\} \\
W^*_{\alpha 3} &= -W^*_{3\alpha} = \frac{1}{8\pi D}(2\ln z-1)rr_{,\alpha} \\
W^*_{33} &= \frac{1}{8\pi D(1-\nu)\lambda^2}[(1-\nu)z^2(\ln z-1)-8\ln z]
\end{aligned} \tag{A1}$$

and

$$\begin{aligned}
P^*_{\gamma\alpha} &= \frac{-1}{4\pi r}[(4A(z)+2zK_1(z)+1-\nu)(\delta_{\alpha\gamma}r_{,n}+r_{,\alpha}n_\gamma) \\
&\quad +(4A(z)+1+\nu)r_{,\gamma}n_\alpha \\
&\quad -2(8A(z)+2zK_1(z)+1-\nu)r_{,\alpha}r_{,\gamma}r_{,n}] \\
P^*_{\gamma 3} &= \frac{\lambda^2}{2\pi}[B(z)n_\gamma - A(z)r_{,\gamma}r_{,n}] \\
P^*_{3\alpha} &= \frac{-(1-\nu)}{8\pi}\left[\left(2\frac{(1+\nu)}{(1-\nu)}\ln z-1\right)n_\alpha+2r_{,\alpha}r_{,n}\right] \\
P^*_{33} &= \frac{-1}{2\pi r}r_{,n}
\end{aligned} \tag{A2}$$

The expression of W^*_{ijk}, P^*_{ijk} and $Q^*_{i\beta}$ are [Vander Weeen (1982)]:

$$\begin{aligned}
W^*_{\alpha\beta\gamma} &= \frac{1}{4\pi r}[(4A(z)+2zK_1(z)+1-\nu) \\
&\quad \times(\delta_{\beta\gamma}r_{,\alpha}+\delta_{\alpha\gamma}r_{,\beta}) \\
&\quad -2(8A(z)+2zK_1(z)+1-\nu)r_{,\alpha}r_{,\beta}r_{,\gamma} \\
&\quad +(4A(z)+1+\nu)\delta_{\alpha\beta}r_{,\gamma}] \\
W^*_{\alpha\beta 3} &= \frac{-(1-\nu)}{8\pi}\left[\left(2\frac{(1+\nu)}{(1-\nu)}\ln z-1\right)\delta_{\alpha\beta}+2r_{,\alpha}r_{,\beta}\right] \\
W^*_{3\beta\gamma} &= \frac{\lambda^2}{2\pi}[B(z)\delta_{\gamma\beta}-A(z)r_{,\gamma}r_{,\beta}] \\
W^*_{3\beta 3} &= \frac{1}{2\pi r}r_{,\beta}
\end{aligned} \tag{A3}$$

$$\begin{aligned}
P^*_{\alpha\beta\gamma} &= \frac{D(1-\nu)}{4\pi r^2}\{(4A(z)+2zK_1(z)+1-\nu) \\
&\quad \times(\delta_{\gamma\alpha}n_\beta+\delta_{\gamma\beta}n_\alpha) \\
&\quad +(4A(z)+1+3\nu)\delta_{\alpha\beta}n_\gamma-(16A(z)+6zK_1(z) \\
&\quad +z^2K_0(z)+2-2\nu) \\
&\quad \times[(n_\alpha r_{,\beta}+n_\beta r_{,\alpha})r_{,\gamma}+(\delta_{\gamma\alpha}r_{,\beta}+\delta_{\gamma\beta}r_{,\alpha})r_{,n}] \\
&\quad -2(8A(z)+2zK_1(z)+1+\nu) \\
&\quad \times(\delta_{\alpha\beta}r_{,\gamma}r_{,n}+n_\gamma r_{,\alpha}r_{,\beta}) \\
&\quad +4(24A(z)+8zK_1(z)+z^2K_0(z)+2-2\nu) \\
&\quad \times r_{,\alpha}r_{,\beta}r_{,\gamma}r_{,n}\} \\
P^*_{\alpha\beta 3} &= \frac{D(1-\nu)\lambda^2}{4\pi r}[(2A(z)+zK_1(z))(r_{,\beta}n_\alpha+r_{,\alpha}n_\beta) \\
&\quad -2(4A(z)+zK_1(z))r_{,\alpha}r_{,\beta}r_{,n}+2A(z)\delta_{\alpha\beta}r_{,n}] \\
P^*_{3\beta\gamma} &= \frac{-D(1-\nu)\lambda^2}{4\pi r}[(2A(z)+zK_1(z))(\delta_{\gamma\beta}r_{,n}+r_{,\gamma}n_\beta) \\
&\quad +2A(z)n_\gamma r_{,\beta}-2(4A(z)+zK_1(z))r_{,\gamma}r_{,\beta}r_{,n}] \\
P^*_{3\beta 3} &= \frac{D(1-\nu)\lambda^2}{4\pi r^2}\left[(z^2B(z)+1)n_\beta\right. \\
&\quad \left.-(z^2A(z)+2)r_{,\beta}r_{,n}\right]
\end{aligned} \tag{A4}$$

$$\begin{aligned}
Q^*_{\alpha\beta} &= \frac{-r}{64\pi}\{(4\ln z-3)[(1-\nu)(r_{,\beta}n_\alpha+r_{,\alpha}n_\beta) \\
&\quad +(1+3\nu)\delta_{\alpha\beta}r_{,n}]+4[(1-\nu)r_{,\alpha}r_{,\beta}+\nu\delta_{\alpha\beta}]r_{,n}\} \\
Q^*_{3\beta} &= \frac{1}{8\pi}[(2\ln z-1)n_\beta+2r_{,\beta}r_{,n}]
\end{aligned} \tag{A5}$$

where

$$\begin{aligned}
A(z) &= K_0(z)+\frac{2}{z}\left[K_1(z)-\frac{1}{z}\right] \\
B(z) &= K_0(z)+\frac{1}{z}\left[K_1(z)-\frac{1}{z}\right]
\end{aligned} \tag{A6}$$

in which $K_0(z)$ and $K_1(z)$ are modified Bessel functions of the second kind [Abramowitz and Stegun (1965)], $z=\lambda r$, λ is the shear factor defined in section 2, r is the absolute distance between the source and the field points, $r_{,\alpha}=r_\alpha/r$, where $r_\alpha = x_\alpha(\mathbf{x})-x_\alpha(\mathbf{x}')$ and $r_{,n}=r_{,\alpha}n_\alpha$.

Expanding the modified Bessel functions for small argu-

ments:

$$K_0(z) = \left[-\gamma - \ln(\frac{z}{2})\right] + \left[-\gamma + 1 - \ln(\frac{z}{2})\right] \frac{(z^2/4)}{(1!)^2} + \left[-\gamma + 1 + \frac{1}{2} - \ln(\frac{z}{2})\right] \frac{(z^2/4)^2}{(2!)^2} + \left[-\gamma + 1 + \frac{1}{2} + \frac{1}{3} - \ln(\frac{z}{2})\right] \frac{(z^2/4)^3}{(3!)^2} + \cdots \tag{A7}$$

$$K_1(z) = \frac{1}{z} - \left[-\gamma + \frac{1}{2} - \ln(\frac{z}{2})\right] \frac{(z^2/4)^{1/2}}{0!1!} - \left[-\gamma + 1 + \frac{1}{4} - \ln(\frac{z}{2})\right] \frac{(z^2/4)^{3/2}}{1!2!} - \left[-\gamma + 1 + \frac{1}{2} + \frac{1}{6} - \ln(\frac{z}{2})\right] \frac{(z^2/4)^{5/2}}{2!3!} + \cdots \tag{A8}$$

where $\gamma = 0.5772156649$ is the Euler constant. Substitute equations (A7 − A8) into (A6) and take the limit as $r \to 0$:

$$\lim_{r\to 0} A(z) = \frac{-1}{2}, \qquad \lim_{r\to 0} B(z) = -\frac{1}{2}\left[\lim_{r\to 0} \ln(\frac{z}{2}) + \gamma + \frac{1}{2}\right] \tag{A9}$$

As it can be seen, $A(z)$ is a smooth function, whereas, $B(z)$ is a weakly singular $O(\ln r)$. Therefore W^*_{ij} is weakly singular and P^*_{ij} has a strong (Cauchy principal value) singularity $O(1/r)$.

In this work, the modified Bessel functions are evaluated using polynomial approximations given by [Abramowitz and Stegun (1965)] .

Appendix A:.2 Two-dimensional Plane Stress Problem

The expressions for the kernels $U^*_{\theta\alpha}$ and $T^*_{\theta\alpha}$ are well known (Kelvin solution) for two-dimensional plane stress problems, and are given as:

$$U^*_{\theta\alpha} = \frac{1}{4\pi B(1-\nu)}\left[(3-\nu)\ln\left(\frac{1}{r}\right)\delta_{\theta\alpha} + (1+\nu) r_{,\theta} r_{,\alpha}\right] \tag{A10}$$

$$T^*_{\theta\alpha} = -\frac{1}{4\pi r}\{r_{,n}[(1-\nu)\delta_{\theta\alpha} + 2(1+\nu) r_{,\theta} r_{,\alpha}] + (1-\nu)[n_\theta r_{,\alpha} - n_\alpha r_{,\theta}]\} \tag{A11}$$

where $U^*_{\theta\alpha}$ are weakly singular kernels of order $O(\ln\frac{1}{r})$ and $T^*_{\theta\alpha}$ are strongly singular in order $O(1/r)$.

The expressions for the kernels $U^*_{\alpha\beta\gamma}$ and $T^*_{\alpha\beta\gamma}$ are :

$$U^*_{\alpha\beta\gamma} = \frac{1}{4\pi r}\left[(1-\nu)\left(\delta_{\gamma\alpha} r_{,\beta} + \delta_{\gamma\beta} r_{,\alpha} - \delta_{\alpha\beta} r_{,\gamma}\right) + 2(1+\nu) r_{,\alpha} r_{,\beta} r_{,\gamma}\right] \tag{A12}$$

$$T^*_{\alpha\beta\gamma} = \frac{B(1-\nu)}{4\pi r^2}\{2r_{,n}[(1-\nu)\delta_{\alpha\beta} r_{,\gamma} + \nu\left(\delta_{\gamma\alpha} r_{,\beta} + \delta_{\gamma\beta} r_{,\alpha}\right) - 4(1+\nu) r_{,\alpha} r_{,\beta} r_{,\gamma}] + 2\nu\left(n_\alpha r_{,\beta} r_{,\gamma} + n_\beta r_{,\alpha} r_{,\gamma}\right) + (1-\nu)\left(2n_\gamma r_{,\alpha} r_{,\beta} + n_\beta \delta_{\alpha\gamma} + n_\alpha \delta_{\beta\gamma}\right) - (1-3\nu) n_\gamma \delta_{\alpha\beta}\} \tag{A13}$$

Appendix B: Particular solutions

Particular solutions derived by [Wen, Aliabadi and Young (2000)] are used for the dual reciprocity technique in this work and are given in the following sections.

Appendix B:.1 Particular solutions for plate bending

Governing equation for shear deformable plate bending problem can be written as

$$\hat{\mathbf{w}} = \mathbf{H}\mathbf{e}\varphi \tag{B1}$$

where particular solutions of displacement $\hat{\mathbf{w}} = \{\hat{w}_1, \hat{w}_2, \hat{w}_3\}^\top$, $\mathbf{e} = \{e_1, e_2, e_3\}^\top$ is arbitrary constant vector and components of matrix $\mathbf{H}$ are

$$H_{\alpha\beta} = 2\delta_{\alpha\beta}\bigtriangledown^4 - [(1+\nu)\bigtriangledown^2 + (1-\nu)\lambda^2)]\frac{\partial^2}{\partial x_\alpha \partial x_\beta}$$

$$H_{3\alpha} = -H_{\alpha 3} = -(1-\nu)(\bigtriangledown^2 - \lambda^2)\frac{\partial}{\partial x_\alpha}$$

$$H_{33} = (\bigtriangledown^2 - \lambda^2)[2\bigtriangledown^2 - (1-\nu)\lambda^2]/\lambda^2 \tag{B2}$$

The function φ can be defined from equation (B1) such that

$$D(1-\nu)(\bigtriangledown^2 - \lambda^2)\bigtriangledown^4 \varphi + F(r) = 0 \tag{B3}$$

If $e_1 = 0, e_2 = 0$ and $e_3 = 1$, the particular solution used in equations (36-38) can be written as

$$\hat{w}_{m\alpha} = -\frac{1}{D}\frac{\partial \psi}{\partial x_\alpha}$$

$$\hat{w}_{m3} = \frac{1}{(1-\nu)D\lambda^2}[2\bigtriangledown^2 \psi - (1-\nu)\lambda^2 \psi] \tag{B4}$$

where

$$\bigtriangledown^4\psi(r)+F(r)=0 \tag{B5}$$

The particular solutions of moment and shear force can be determined from the stress resultant-displacement relationship for shear deformable plate bending. The tractions on the boundary can be obtained by

$$\hat{p}_{m\alpha}=\hat{M}_{\alpha\beta}n_\beta,\ \ \hat{p}_{m3}=\hat{Q}_\alpha n_\alpha \tag{B6}$$

If radial basis function $F(r)=1+r$, The function $\psi(r)$ can be solved from equation (B5)

$$\psi(r)=-\left(\frac{r^4}{64}+\frac{r^5}{225}\right) \tag{B7}$$

and the rotations and deflection can be deduced

$$\begin{aligned}
\hat{w}^3_{m1}&=-\left(\frac{1}{16}+\frac{r}{45}\right)\frac{x_1r^2}{D}\\
\hat{w}^3_{m2}&=-\left(\frac{1}{16}+\frac{r}{45}\right)\frac{x_2r^2}{D}\\
\hat{w}^3_{m3}&=-\left(\frac{1}{2}+\frac{2r}{9}\right)\frac{r^2}{(1-\nu)\lambda^2D}+\left(\frac{1}{64}+\frac{r}{225}\right)\frac{1}{D}
\end{aligned} \tag{B8}$$

The particular solutions of moments $\hat{M}_{\alpha\beta}$ and shear forces $\hat{Q}_\beta$ can be determined by the stress resultant-displacement relationship for shear deformable plate bending to give

$$\begin{aligned}
\hat{M}^3_{m11}&=-\left[\left(\frac{1}{8}+\frac{r}{15}\right)\left(x_1^2+\nu x_2^2\right)+(1+\nu)\left(\frac{r^2}{16}+\frac{r^3}{45}\right)\right]\\
\hat{M}^3_{m12}&=-(1+\nu)\left(\frac{1}{8}+\frac{r}{15}\right)(x_1x_2)\\
\hat{M}^3_{m22}&=-\left[\left(\frac{1}{8}+\frac{r}{15}\right)\left(\nu x_1^2+x_2^2\right)+(1+\nu)\left(\frac{r^2}{16}+\frac{r^3}{45}\right)\right]
\end{aligned} \tag{B9}$$

$$\begin{aligned}
\hat{Q}^3_{m1}&=-\frac{x_1}{2}\left(1+\frac{2r}{3}\right)\\
\hat{Q}^3_{m2}&=-\frac{x_2}{2}\left(1+\frac{2r}{3}\right)
\end{aligned}$$

and the tractions on the boundary can be obtained from relationships in equation (B6).

For the derivative of function $F_{,\alpha}=x_\alpha/r$, the solution $\psi^\alpha(r)$ can be found

$$\psi^\alpha(r)=-\frac{r^3x_\alpha}{45} \tag{B10}$$

and particular solutions $\hat{w}^\alpha_{mk}$ are

$$\begin{aligned}
\hat{w}^1_{m1}&=-(3x_1^2+r^2)\frac{r}{45D}\\
\hat{w}^1_{m2}&=-\frac{x_1x_2r}{15D}\\
\hat{w}^1_{m3}&=-[30-(1-\nu)\lambda^2r^2]\frac{rx_1}{45(1-\nu)\lambda^2D}
\end{aligned} \tag{B11}$$

and the particular solutions of moments $\hat{M}_{\alpha\beta}$ and shear forces $\hat{Q}_\beta$ are

$$\begin{aligned}
\hat{M}^1_{m11}&=-\frac{x_1}{15}\left[\nu\left(\frac{x_1^2}{r}+3r\right)+\left(\frac{x_2^2}{r}+r\right)\right]\\
\hat{M}^1_{m12}&=-(1-\nu)\frac{x_2}{15}\left(\frac{x_1^2}{r}+r\right)\\
\hat{M}^1_{m22}&=-\frac{x_1}{15}\left[\nu\left(\frac{x_1^2}{r}+3r\right)+\left(\frac{x_2^2}{r}+r\right)\right]\\
\hat{Q}^1_{m1}&=-\frac{1}{3}\left(\frac{x_1^2}{r}+r\right)\\
\hat{Q}^1_{m2}&=-\frac{1}{3}\frac{x_1x_2}{r}
\end{aligned} \tag{B12}$$

for $\alpha=1$, and

$$\begin{aligned}
\hat{w}^2_{m1}&=-\frac{x_1x_2r}{15D}\\
\hat{w}^2_{m1}&=-(3x_2^2+r^2)\frac{r}{45D}\\
\hat{w}^2_{m3}&=-[30-(1-\nu)\lambda^2r^2]\frac{rx_2}{45(1-\nu)\lambda^2D}
\end{aligned} \tag{B13}$$

and the particular solutions of moments $\hat{M}_{\alpha\beta}$ and shear forces $\hat{Q}_\beta$ are

$$\begin{aligned}
\hat{M}^2_{m11}&=-\frac{x_2}{15}\left[\nu\left(\frac{x_1^2}{r}+r\right)+\left(\frac{x_2^2}{r}+3r\right)\right]\\
\hat{M}^2_{m12}&=-(1-\nu)\frac{x_1}{15}\left(\frac{x_2^2}{r}+r\right)\\
\hat{M}^2_{m22}&=-\frac{x_2}{15}\left[\nu\left(\frac{x_1^2}{r}+r\right)+\left(\frac{x_2^2}{r}+3r\right)\right]\\
\hat{Q}^2_{m1}&=-\frac{1}{3}\frac{x_1x_2}{r}\\
\hat{Q}^2_{m2}&=-\frac{1}{3}\left(\frac{x_2^2}{r}+r\right)
\end{aligned} \tag{B14}$$

for $\alpha=2$.

Appendix B:.2 Particular solutions for two-dimensional plane stress

An expression displacement particular solution $\hat{u}^{\gamma}_{m\alpha}$ can be found in polar coordinates with the use of the Galerkin vector $G_{\alpha\beta}$ as

$$\hat{u}^{\gamma}_{m\alpha}(r) = G^{\gamma}_{\beta\alpha,\gamma\gamma}(r) - \frac{1+\nu}{2} G^{\gamma}_{\gamma\alpha,\beta\gamma}(r) \tag{B15}$$

where $G_{\alpha\beta}$ satisfies

$$\bigtriangledown^4 G^{\gamma}_{\beta\alpha} + \frac{2}{(1-\nu)B}\frac{x_{\gamma}}{r}\delta_{\gamma\beta} = 0 \tag{B16}$$

and a solution is determined by

$$G^{\gamma}_{\beta\alpha} = -\frac{r^3 x_{\gamma}}{45\,(1-\nu)\,B}\delta_{\alpha\beta} \tag{B17}$$

Substituting equation (B17) into equation (B15), then the displacement particular solutions can be arranged as

$$\hat{u}^1_{m1} = -\frac{2}{(1-\nu)B}\left[\frac{r x_1}{3} - \frac{1+\nu}{30}\left(\frac{x_1^3}{r} + 3x_1 r\right)\right]$$

$$\hat{u}^1_{m2} = \frac{(1+\nu)}{15(1-\nu)B}\left(\frac{x_1^2 x_2}{r} + x_2 r\right) \tag{B18}$$

and using strain displacement relationships for two-dimensional plane stress, the strain are obtained as

$$\hat{\varepsilon}^1_{m11} = -\frac{2}{(1-\nu)}\left[\left(\frac{x_1^2}{r} + \frac{r}{3}\right) - \frac{1+\nu}{30}\left(-\frac{x_1^4}{r^3} + \frac{6x_1^2}{r} + 3r\right)\right]$$

$$\hat{\varepsilon}^1_{m12} = -\frac{2}{(1-\nu)}\left[\frac{x_1 x_2}{6r} - \frac{1+\nu}{30}\left(-\frac{x_1^3 x_2}{r^3} + \frac{3x_1 x_2}{r}\right)\right]$$

$$\hat{\varepsilon}^1_{m22} = \frac{2}{(1-\nu)}\frac{1+\nu}{30}\left(-\frac{x_1^2 x_2^2}{r^3} + 2r\right) \tag{B19}$$

The particular solution for membrane stress resultant can be derived by substituting equation (B19) into the stress resultant-strain relationships for two-dimensional plane stress to give:

$$\hat{N}^1_{m11} = B\left[(1-\nu)\hat{\varepsilon}^1_{m11} + \nu\hat{\varepsilon}^1_{m\alpha\alpha}\right]$$

$$\hat{N}^1_{m12} = B(1-\nu)\hat{\varepsilon}^1_{m12}$$

$$\hat{N}^1_{m22} = B\left[(1-\nu)\hat{\varepsilon}^1_{m22} + \nu\hat{\varepsilon}^1_{m\alpha\alpha}\right] \tag{B20}$$

and the traction particular solutions are obtained from

$$\hat{t}^1_{m\alpha} = \hat{N}^1_{m\alpha\beta} n_{\beta} \tag{B21}$$

In the same way, displacement particular solutions $\hat{u}^2_{m\alpha}$ can be obtained as follows:

$$\hat{u}^2_{m1} = \frac{(1+\nu)}{15(1-\nu)B}\left(\frac{x_2^2 x_1}{r} + x_1 r\right)$$

$$\hat{u}^2_{m2} = -\frac{2}{(1-\nu)B}\left[\frac{r x_2}{3} - \frac{1+\nu}{30}\left(\frac{x_2^3}{r} + 3x_2 r\right)\right] \tag{B22}$$

and the strains are

$$\hat{\varepsilon}^2_{m11} = \frac{2}{(1-\nu)}\frac{1+\nu}{30}\left(-\frac{x_1^2 x_2^2}{r^3} + 2r\right)$$

$$\hat{\varepsilon}^2_{m12} = -\frac{2}{(1-\nu)}\left[\frac{x_1 x_2}{6r} - \frac{1+\nu}{30}\left(-\frac{x_2^3 x_1}{r^3} + \frac{3x_1 x_2}{r}\right)\right]$$

$$\hat{\varepsilon}^2_{m22} = -\frac{2}{(1-\nu)}\left[\left(\frac{x_2^2}{r} + \frac{r}{3}\right) - \frac{1+\nu}{30}\left(-\frac{x_2^4}{r^3} + \frac{6x_2^2}{r} + 3r\right)\right] \tag{B23}$$

The particular solution for membrane stress resultant are

$$\hat{N}^2_{m11} = B\left[(1-\nu)\hat{\varepsilon}^2_{m11} + \nu\hat{\varepsilon}^2_{m\alpha\alpha}\right]$$

$$\hat{N}^2_{m12} = B(1-\nu)\hat{\varepsilon}^2_{m12}$$

$$\hat{N}^2_{m22} = B\left[(1-\nu)\hat{\varepsilon}^2_{m22} + \nu\hat{\varepsilon}^2_{m\alpha\alpha}\right] \tag{B24}$$

and finally the traction particular solutions are obtained from

$$\hat{t}^2_{m\alpha} = \hat{N}^2_{m\alpha\beta} n_{\beta} \tag{B25}$$